

# Software Customization to Provide Digital Oscilloscope With Enhanced Period-Measurement Features

Maria Grazia D'Elia, Consolatina Liguori, *Member, IEEE*, Vincenzo Paciello, and Antonio Pietrosanto, *Member, IEEE*

**Abstract**—This paper tackles the problem of signal period measurements by means of oscilloscopes. First, the performance of two last-generation scopes, implementing a zero-crossing algorithm, is evaluated. Then, after a brief resume of alternative measurement techniques, a solution to enhance the period-measurement capability of scopes is proposed and implemented in the LeCroy WaveMaster 8620A software. Finally, the results of the tests carried out on different signal waveforms are reported and analyzed.

**Index Terms**—Digital instrument, digital signal processing, level-crossing problems, period measurement, uncertainty evaluation.

## I. INTRODUCTION

THE NEWEST developments in analog front end and trigger circuit bandwidth (up to 10 GHz), as well as in analog-to-digital converter (ADC) sampling rate (20 Gsample/s), have produced, together with long dynamic random access memory (DRAM) data rates (up to 20 GB/s), significant advances in the realization of high-performance hardware platforms for digital oscilloscopes [1]–[4]. Moreover, on-board digital signal processing has made oscilloscopes evolve into the most valuable tool utilized in the development of all forms of electronic equipment.

Digital signal processing has been getting increasingly widespread during the last decade, thanks to the availability of *ad hoc* processors [the so-called digital signal processors (DSP)], which offer high computational power at acceptable cost. Electronic instruments, including DSP, can see both their performance and their features rise significantly.

Oscilloscopes, in particular, can use the power of digital signal processing both to implement amplitude and frequency-domain measurement options and to increment acquired-sample resolution by suitable algorithms.

In order to successfully reach these goals, granting that the quality of measurements be comparable with the cost of very high-performance instruments, the implemented algorithms should be both robust versus measurement parameters, and fast in run time. Their sensitivity to either user-defined or incon-

trollable parameters, like sampling frequency, record length, signal waveform, and noise level, should be minimum. At the same time, the computational burden should be so low that the response time still be acceptable also in case of acquisitions characterized by fast time base and high record length.

It is really difficult to believe that the tradeoff between these opposite needs can be achieved by manufacturers for all measurement functions (rms, peak, period, frequency, rise time, etc.) provided by oscilloscopes. The manufacturer's choice usually falls on algorithms mainly characterized by low computational burden that assures proper working in the most common conditions, thus, accepting that they may be inadequate in some boundary cases. The problem is that oscilloscope manufacturers rarely give information about this boundary as well as they do for measurement accuracy. The consequence is that users who want to know the actual limits and performance of the oscilloscope measurement algorithms must do them by themselves. The method of exhaustive verification is often hard to be run, since the numerous measurement parameters to be explored would require a very high number of tests. This means that users must trust their measurement expertise to detect, during the daily use of the instrument, rough errors due to limited performance of some signal processing algorithms.

On the other hand, thanks to the choice of all major oscilloscope manufacturers of substituting on-board installed proprietary operating systems [1]–[4] with the widespread Microsoft Windows, measurement software features today could be increased by the user.

Some of the last generation of oscilloscopes, in fact, allow creating custom parameter measurements or math functions in the scope's user interface. Unique or proprietary MATLAB, Mathcad, VBScript, or even Excel calculations can be selected like any other installed parameter or math function, and the results displayed on the scope screen. These features can be used to add new measurement functions that can be recalled by the user in those cases where evident limits of the default measurement functions have been highlighted.

In this framework, the authors have tested the top-level products of Tektronix and LeCroy in the period measurement of typical signals, exploring parameters like: noise level, number of periods, and number of samples acquired in the period. Both scopes adopt a simple zero-crossing method, which is not applicable to all waveforms. In this paper, the test results are widely discussed.

Manuscript received June 15, 2004; revised December 20, 2005.

The authors are with the Department of Information Engineering and Electric Engineering, University of Salerno, 84084 Fisciano, Italy (e-mail: mgdelia@unisa.it; tliguori@unisa.it; vpaciello@unisa.it; apietrosanto@unisa.it).

Digital Object Identifier 10.1109/TIM.2006.870128

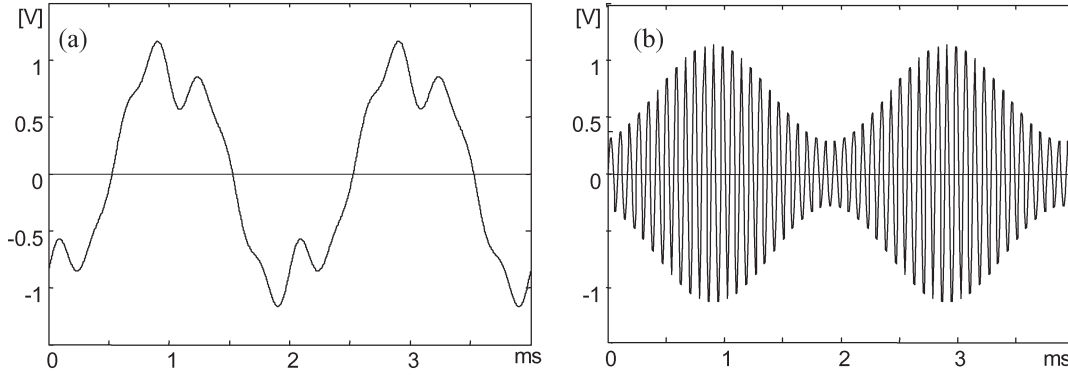


Fig. 1. Signal with (a) one and (b) more than one zero crossing for period.

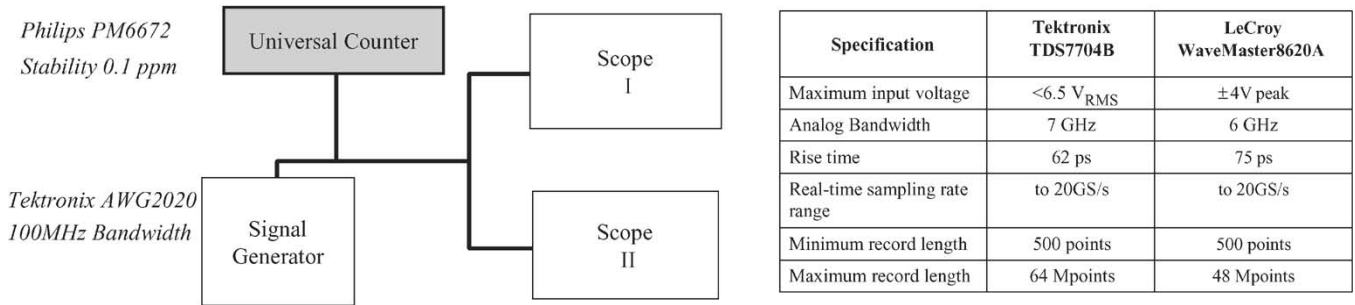


Fig. 2. Test measurement station and digital scope specifications.

Then, after a brief resume of some algorithms proposed in literature, it is described how the XDEV advanced customization package has been utilized to provide the LeCroy WaveMaster 8620 A 6-GHz digital oscilloscope, with a more robust and accurate period-measurement algorithm. The new period measurement function was obtained by a suitable upgrade of the algorithm proposed in [13] by Schoukens *et al.* The software has been written in Virtual Basic Scripts. The automation language has allowed device commands to be sent to the scope, and ActiveX functions have been used to manage the on-screen output. Finally, the performance of the customer-made new period measurement function is evaluated in terms of uncertainty and response time.

II. PERIOD MEASUREMENTS WITH SCOPE

The period  $T_x$  of a periodic signal  $x(t)$  is defined as the time interval after which the signal replays itself.

$$x(t + T_x) = x(t) \quad \forall t. \tag{1}$$

In the practice, (1) is never verified because of both the presence of noise and finite length of the observation window  $\Delta T$ . Consequently, the period should be defined as

$$x(t + T_x) \cong x(t) \quad \forall t \in \Delta T. \tag{2}$$

Many approaches, also hybrid and/or multistages, are reported in literature for the period measurement of digitized signals. In most of them, a first analysis gives a rough estimation of the period, while a further algorithm improves the measurement accuracy.

The **zero-crossing methods** [6], [7] evaluate the period of sampled signals as the time distance between two consecutive crossings of a trigger level (usually zero) with the same slope [see Fig. 1(a)]. This is the method adopted by most of the scopes. It requires very low computational burden, but is not applicable to signals with more than one zero crossing for the period [see Fig. 1(b)], and its accuracy depends on the signal-to-noise ratio. An accuracy enhancement can be achieved if the zero-crossing detection phase starts after the signal has been preprocessed (e.g., filtered) [5]. Since preprocessing might strictly depend on the signal characteristics, the solution is rarely implemented on oscilloscopes. On the contrary, they often adopt a tunable hysteresis threshold to reduce the zero-crossing noise sensitivity with no additional burden.

In order to evaluate the limits and accuracy of the scope period measurements, the top-level products of two leader scope manufacturers (Tektronix and LeCroy), both adopting a zero-crossing algorithm, were tested on period measurements (see Fig. 2). The test measurement station was completed by a polynomial arbitrary waveform generator and a digital counter as period-measurement reference. Measurements were made on different waveforms [sinusoid, square, triangle, AM modulated, FM modulated, pulsewidth modulation (PWM), and so on], with and without Gaussian noise, and different sampling time to signal-period ratio. As it was expected, both the oscilloscopes completely failed the period measurement of AM and FM signals, in which the period cannot be evaluated with a zero-crossing method. Test results were identical for both scopes: They measured the carrier period of the AM signals and a period value depending on synchronization for FM signals. As for waveforms with one zero crossing per period (said

TABLE I  
PERIOD-MEASUREMENT RESULTS

Signal input		Tektronik 7704B				LeCroy WaveMaster 8620A			
Waveform	noise/signal	$N_t$	$N_p$	$\mu_T$	$u_T$	$N_t$	$N_p$	$\mu_T$	$u_T$
Sinusoidal	0.05%	2500	250	998.9 $\mu$ s	2.4 $\mu$ s	2500	250	999.6 $\mu$ s	2.1 $\mu$ s
	2.5%			998.8 $\mu$ s	2.3 $\mu$ s			1000.0 $\mu$ s	2.0 $\mu$ s
	0.05%	5000	250	998.67 $\mu$ s	1.7 $\mu$ s	5000	250	999.8 $\mu$ s	2.1 $\mu$ s
	2.5%			998.8 $\mu$ s	2.8 $\mu$ s			999.8 $\mu$ s	2.8 $\mu$ s
	0.05%	5000	500	998.9 $\mu$ s	2.1 $\mu$ s	5000	500	1000.0 $\mu$ s	2.0 $\mu$ s
	2.5%			999.3 $\mu$ s	1.7 $\mu$ s			999.9 $\mu$ s	1.6 $\mu$ s
Triangular	0.05%	2500	250	998.9 $\mu$ s	3.1 $\mu$ s	2500	250	1001.0 $\mu$ s	3.0 $\mu$ s
	2.5%			999.6 $\mu$ s	3.3 $\mu$ s			1001.0 $\mu$ s	4.0 $\mu$ s
	0.05%	5000	250	998.1 $\mu$ s	2.6 $\mu$ s	5000	250	1000.0 $\mu$ s	3.0 $\mu$ s
	2.5%			998.5 $\mu$ s	3.8 $\mu$ s			1001.0 $\mu$ s	4.0 $\mu$ s
	0.05%	5000	500	999.1 $\mu$ s	2.2 $\mu$ s	5000	500	1000.0 $\mu$ s	3.0 $\mu$ s
	2.5%			999.1 $\mu$ s	2.7 $\mu$ s			1000.0 $\mu$ s	3.0 $\mu$ s
Square	0.05%	2500	250	1000.013 $\mu$ s	0.004 $\mu$ s	2500	250	999.997 $\mu$ s	0.002 $\mu$ s
	2.5%			999.981 $\mu$ s	0.004 $\mu$ s			999.999 $\mu$ s	0.002 $\mu$ s
	0.05%	5000	250	999.995 $\mu$ s	0.004 $\mu$ s	5000	250	1000.002 $\mu$ s	0.002 $\mu$ s
	2.5%			1000.000 $\mu$ s	0.004 $\mu$ s			1000.008 $\mu$ s	0.002 $\mu$ s
	0.05%	5000	500	999.999 $\mu$ s	0.002 $\mu$ s	5000	500	999.998 $\mu$ s	0.001 $\mu$ s
	2.5%			1000.003 $\mu$ s	0.003 $\mu$ s			999.997 $\mu$ s	0.001 $\mu$ s

canonic waveforms in the following), on the contrary, no rough error was detected. Main data are organized in Table I, where scope period measurements and respective uncertainty  $u$  are reported for different noise levels and number of sample per period. The signal period was kept constant (1.0 ms) in all tests, as evidenced by the counter measurements. The behavior of the two instruments is very similar also in these conditions: Deterministic errors are null in all the cases, while the uncertainty never exceeds 0.3%. In particular, the higher the signal slew rate, the lower the period-measurement uncertainty (square wave,  $u = 0.004\%$ ). Moreover, the 2.5% noise level added to the test signals influences the uncertainty only when the slew rate is minimum (sinusoid). Finally, both the 0.004% uncertainty of the square-wave period measurements and the substantial independence of the uncertainty, by the number of samples per period, lead to suspect that the scope zero-crossing algorithms are followed by an interpolation technique.

### III. HOW TO EXTEND THE PERIOD-MEASUREMENT SCOPE CAPABILITY

The aforementioned results highlighted that the period-measurement capability of scopes is constrained to canonic waveforms by the zero-crossing algorithm. This means that an extension of their capability could be obtained only with alternative measurement techniques. As an example, **frequency-domain** algorithms [8], [9] are based on a preliminary digital Fourier transforms. Then, the searching for peaks of the obtained amplitude-spectrum samples allows all the signal spectrum components to be detected. The fundamental frequency

$f_x$  (and consequently the period  $T_x = 1/f_x$ ) is evaluated analyzing the measured spectrum. Different postprocessing algorithms are proposed in literature: As an example, the fundamental frequency can be defined as the greatest common divisor of the measured frequencies' peaks [see Fig. 3(a)]. All frequency-domain methods require significant computational burden, but are more robust and more general than the zero-crossing ones. Some problems can arise because the scope setup (in terms of time base and record length) is usually driven by time domain rather than frequency-domain specifications.

Some other methods [10]–[13] use the **autocorrelation function**. The autocorrelation  $R(\tau)$  of a waveform gives an indication of similarity of the waveform with its time-shifted  $\tau$  version

$$R(\tau) = \int_{-\infty}^{+\infty} x(t) \cdot x(t + \tau) \cdot dt. \quad (3)$$

Consequently, there is a relative maximum  $R(T_x)$  in the autocorrelation in correspondence to a time shift equal to the period  $T_x$  [see Fig. 3(b)].

These procedures work on a set of  $N$  sampled data  $\{x_n\}$  acquired with a constant sampling period  $T_c$ ,  $x_n = x(nT_c)$ , and the autocorrelation function is calculated as

$$R(n) = \sum_{m=0}^{N-1} x_{n+m} \cdot x_n, \quad \text{for } -(N-1) < n < N-1$$

where  $x_n = 0 \forall n < 0$ , and  $n \geq N$ .

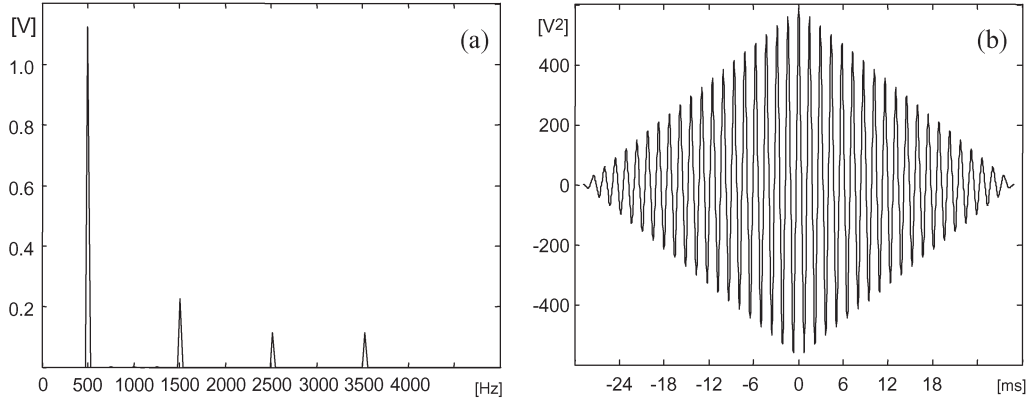


Fig. 3. (a) Amplitude spectrum and (b) autocorrelation function of a signal with more spectral components.

Also, these methods require more processing power than the zero-crossing ones and are more robust and general.

In particular, in [12], Wong-Lam and Naley proposed to precede a zero-crossing interpolated method with an interesting algorithm based on autocorrelation; a normalization function is also suggested to compensate the edge effect due to the limited-time window. Even though based on an interesting approach, this algorithm also fails the period measurement of the modulated signal, because it does not allow removing the peaks in  $R(\tau)$  due to the carrier frequency.

A good solution to this problem was suggested in [13] by Schoukens *et al.* The two-step procedure starts with a rough estimation of the period, also in this case based on the autocorrelation function. Then, the refinement to obtain a precision period measurement is made by a cost function. However, in its whole extension, the procedure carries out a precise period measurement, but it seems too complex to be executed in real time.

On the basis of these considerations, the authors decided to suitably modify the first step of the aforementioned procedure, to obtain an acceptable accuracy in signal-period measurements. Particular care was finally reserved in the implementation to minimize the computational burden and assure a response time suitable for oscilloscope applications.

#### IV. SCOPE IMPLEMENTATION

The method proposed in [13] can be easily summarized.

First, the autocorrelation function  $R(n)$  is evaluated. Then, an iterative procedure begins with the normalization of  $R(n)$ , aiming to evidence the relative maximum in the autocorrelation function corresponding to the time shift proportional to the signal period, through the following rule.

$$R^*(n) = \begin{cases} 1, & \text{if } R(n) \geq th \\ 0, & \text{if } R(n) < th \end{cases} \quad (4)$$

where  $th$  is a fraction of the maximum of  $R(n)$ .

Successively,  $R_g(n)$  is obtained by smoothing  $R^*(n)$  with a Gaussian filter of  $G$ th order [where  $G = \min(N/50, 64)$ ], and its pulse response is

$$g(m) = e^{-(-1+\frac{m}{G})^2}. \quad (5)$$

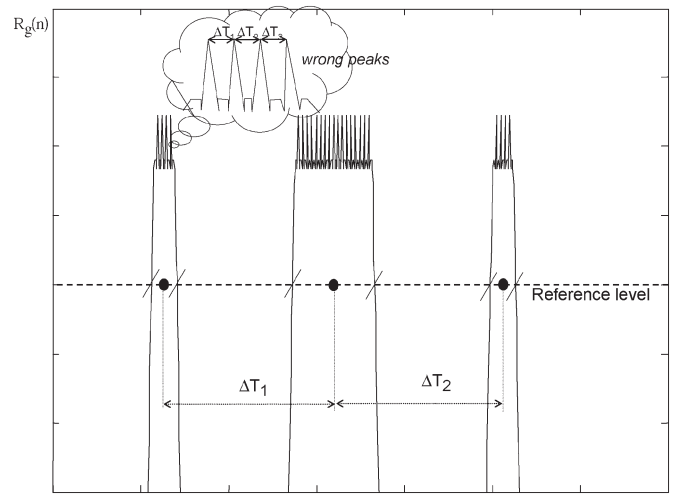


Fig. 4.  $R_g(n)$  for an AM-modulated signal.

Finally, if at least three peaks are detected in  $R_g(n)$ , then the first estimate of the signal period is equal to the median distance between these peaks; otherwise, the  $th$  value has to be decreased, and the procedure is repeated until the three-peak condition is satisfied.

In the second step, an improved estimate of the signal period can be achieved by minimizing the cost function  $V(T)$  defined on the basis of the calculation of the discrete Fourier transform (DFT) spectrum of the samples, resulting in a cubic interpolation of the up-sampled acquired data. The complexity of this step is, if possible, increased by the nonlinearity in  $T$  of the minimization problem that imposes nonlinear search strategies.

Even though appreciating the robustness and the accuracy of the method, the authors found it too onerous if executed up to the second step. A more realistic and useful implementation of this method on the scope was limited to the first step; after that, some aspects of the procedure, conditioning both the accuracy and the computational burden of the first estimate, were revised. In particular, 1) the iterative structure of the procedure was avoided, and 2) the automatic peak-detection problem was resolved.

To avoid the iterative search of  $th$ , tests were made to determine a starting value that satisfies the final condition

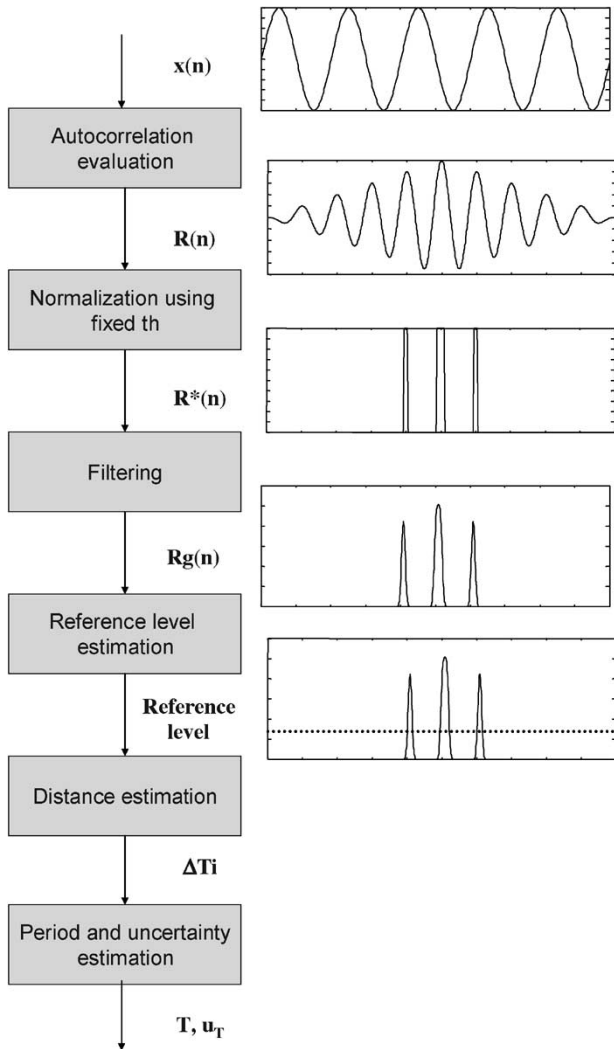


Fig. 5. Whole measurement procedure.

[at least three peaks in  $R_g(n)$ ] for most of the signal waveforms. In particular, for each test condition, the maximum  $th$  value that satisfies the final condition was evaluated. Analyzing these values, the authors found that for record lengths less than 2500 points, the threshold is equal to  $0.71 * \max(R(n))$ , while for greater record lengths, the right value is 0.73.

Especially for AM signals,  $R_g(n)$  looks like the shape reported in Fig. 4. Supposing an automatic peak distance evaluation, two kinds of problems arise. The small peaks on the main lobe could be confused with the main peaks, thus, causing rough errors in the period estimate. Moreover, the uncertainty in the evaluation of the distances between the main peaks is high.

Due to these problems (see Fig. 4), the determination of an amplitude level, which can be crossed by main lobes only, is a crucial task. Such a level (hereinafter called the “reference level”) can be obtained by analyzing the relative maxima amplitude histogram that can assume either a bimodal or a monomodal form in case of the aforementioned noise problems. The reference level is either one half of the minimum amplitude or 80% of the mean, respectively.

The main steps of the complete algorithm are sketched in Fig. 5.

```

%%%%%%%%%%%%%%%%%%%%%%%%%%%%%%%%%%%%%%%%%%%%%%%%%%%%%%%%%%%%%%%%%%%%%%%%
%% Here there were some initializations %
%%%%%%%%%%%%%%%%%%%%%%%%%%%%%%%%%%%%%%%%%%%%%%%%%%%%%%%%%%%%%%%%%%%%%%%%

R=xcorr(WformIn1);
% WformIn1 is the last sample sets acquired by the scope%

R=R/max(R);
Rnormalized=(R>th); % th is the fixed threshold%

%%%%%%%%%%%%%%%%%%%%%%%%%%%%%%%%%%%%%%%%%%%%%%%%%%%%%%%%%%%%%%%%%%%%%%%%
% Rn filtering obtaining Rg %
%%%%%%%%%%%%%%%%%%%%%%%%%%%%%%%%%%%%%%%%%%%%%%%%%%%%%%%%%%%%%%%%%%%%%%%%

G=min(floor(N/50),64);
g=exp(-3*(-1/G:1).^2);
for(n=2*G:length(Rnormalized)-2*G-1,
    Rg(n)=sum(g.*(Rnormalized((n-2*G+1):n+1)));
end;
%%%%%%%%%%%%%%%%%%%%%%%%%%%%%%%%%%%%%%%%%%%%%%%%%%%%%%%%%%%%%%%%%%%%%%%%
% The peaks search
%%%%%%%%%%%%%%%%%%%%%%%%%%%%%%%%%%%%%%%%%%%%%%%%%%%%%%%%%%%%%%%%%%%%%%%%

indexMAx=findpeaks(Rg);

%The reference level determination
Isto = hist(round(Rg(indexMAx)));
AmpPeak = find(Isto ~= 0) ;
if length(AmpPeak) > 2
    th=0.8*(mean(Rg(indexMAx(1:length(indexMAx)))));
else
    th=min(fix(Rg(indiceMAx)))/2;
end

indexPeak=findpeaks_onThreshold(Rg,th);

%%%%%%%%%%%%%%%%%%%%%%%%%%%%%%%%%%%%%%%%%%%%%%%%%%%%%%%%%%%%%%%%%%%%%%%%
% The peak distances (DeltaTi) evaluation
%%%%%%%%%%%%%%%%%%%%%%%%%%%%%%%%%%%%%%%%%%%%%%%%%%%%%%%%%%%%%%%%%%%%%%%%
i=0;
for n=1:2:(length(indexPeak)-1)
    i=i+1;
    DTi(i) = indexPeak (n) + (indexPeak (n+1)- indexPeak (n))/2;
end

PeriodInNumber=median(DTi);
T= periodInNumber*Ts; % Ts is the sampling period
uT=Ts/sqrt(3*length( Ti));
    
```

Fig. 6. Sketch of the MATLAB software.

### A. Uncertainty Evaluation

First, some simulations were carried out in order to evidence the systematic effects on the period measurement. To this aim, numerous combinations among measurement parameters (record length, time base) and signal characteristics (waveform, signal period, noise level) have been explored. No significant deterministic effects were detected. Then, an analytical approach was followed in order to estimate the uncertainty. In particular, the period is evaluated as

$$T_m = \frac{\sum_{i=1}^N \Delta T_i}{N - 1} \quad (6)$$

where  $\Delta T_i$  are the measured distances between the peaks, and  $N$  is the number of detected peaks.

Applying the Guide to the Expression of Uncertainty in Measurement (GUM), published by ISO, procedure to the

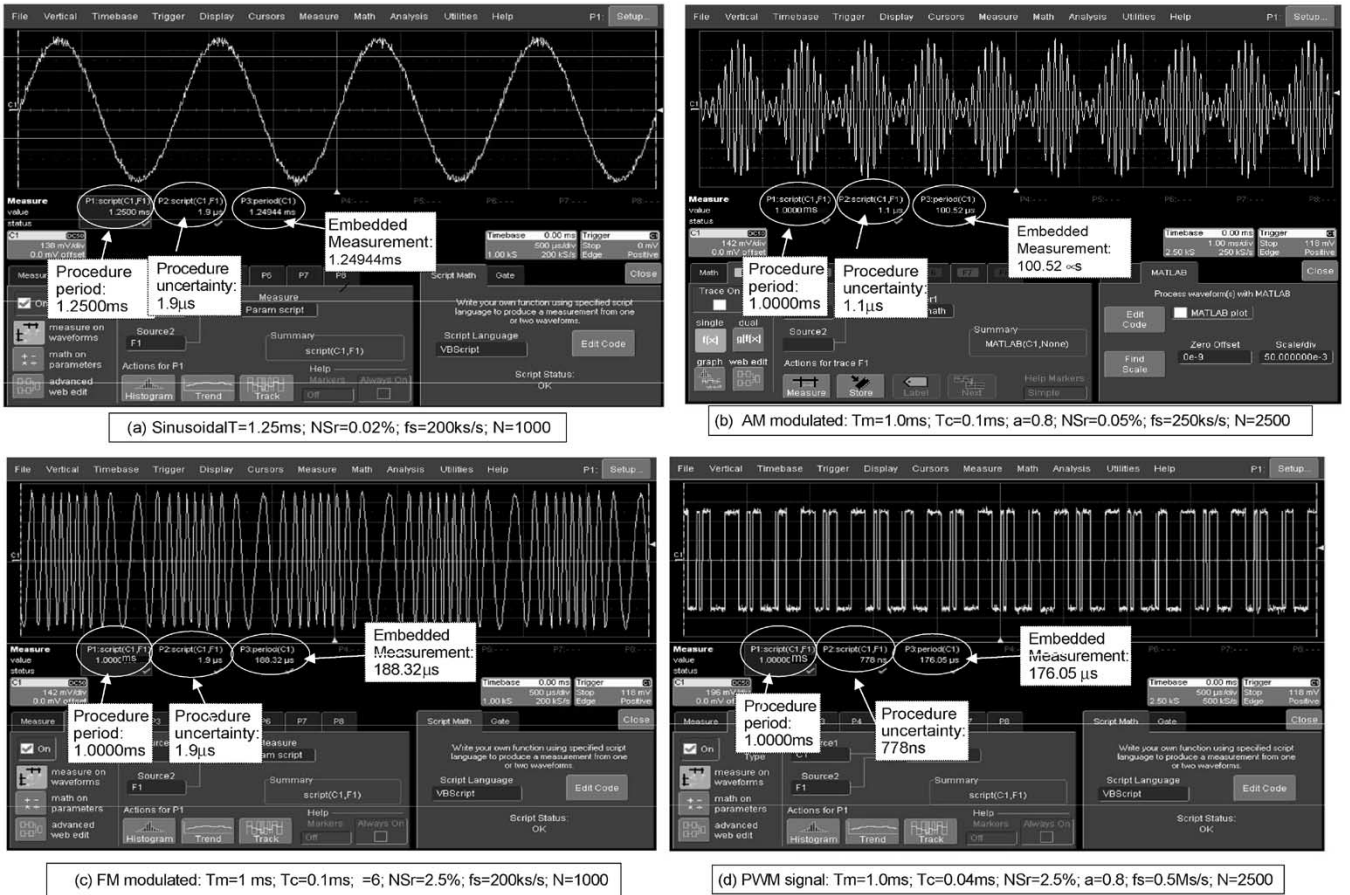


Fig. 7. Scope screen displayed for different waveforms and configurations:  $T$  = signal period,  $\text{NSr}$  = noise to signal percentage,  $f_s$  = scope sampling frequency,  $N$  = number of acquired sample,  $T_m$  = modulating period,  $T_c$  = carried period,  $a$  = AM modulation factor,  $\beta$  = FM modulation factor.

relationship (6), and considering uncorrelated estimations  $\Delta T_i$ , we have

$$\begin{aligned}
 u_{T_m}^2 &= \sum_{i=1}^{N-1} \left( \frac{\partial T_m}{\partial \Delta T_i} \right)^2 \cdot u_{\Delta T_i}^2 \\
 &= \sum_{i=1}^{N-1} \left( \frac{1}{N-1} \right)^2 \cdot u_{\Delta T_i}^2 \\
 &= \frac{u_{\Delta T_i}^2}{N-1}.
 \end{aligned} \quad (7)$$

Only the resolution, the sampling period  $T_s$ , gives its contribution to the  $\Delta T_i$  uncertainty. The result is that, considering a uniform distribution, we have  $u_{\Delta T_i} = T_s/\sqrt{3}$ , and consequently

$$u_{T_m} = \frac{T_s}{\sqrt{(N-1) \cdot 3}}. \quad (8)$$

### B. Algorithm Codification

The algorithm was implemented in MATLAB, with which the signal processing toolbox offers a set of primitive functions to speed up the software development and assure optimized coding. Furthermore, the interaction between the MATLAB workspace and the LeCroy scope memory is made very easy by suitable commands that can be directly included in the

MATLAB code [14]. In Fig. 6, a sketch of the MATLAB code implementing the period measurement is shown; as you can see, the points acquired by the scope can be used as a workspace variable (`WformIn1`). The period-measurement results are presented in suitable parameter windows activated by means of VBScript (see Fig. 7).

### C. Experimental Tests

In Table II, the measurements of the canonic-waveform period are reported. As it can be noted, the uncertainty is comparable with the zero-crossing-method uncertainty, but any influence of the signal slew rate is detected.

Fig. 7 shows some scope screen images where both the measurement function outputs are displayed. Particular attention should be paid to Fig. 7 (b)–(d), which deals with those signals, where the zero-crossing algorithm fails. On the contrary, the measurement results provided by the author software are always correct and characterized by a reasonable uncertainty.

Finally, a comparison in terms of execution time was also made. As it was expected, the measurement procedure implemented by the authors requires an additional burden with respect to the scope embedded measurement function, and its execution time depends on the record length (the number of processed samples  $N$ ). See Table III, where some measured execution times are summarized. However, this rate reduction

TABLE II  
MEAN AND STANDARD DEVIATION (ON A SET OF 32 SAMPLES) OF PERIOD MEASUREMENTS  
FOR TRADITIONAL WAVEFORMS IN CASE OF SYNCHRONOUS SAMPLING

Waveform	noise/signal	Record	Ts [μs]	$\mu_T$ [μs]	$\sigma_T$ [μs]
Sinusoidal $T_x=1000.8105\mu s \pm 0.0005\mu s$	0.05%	2500	40	1000.95	0.21
	2.5%			1000.68	0.46
	0.05%	5000	40	1000.03	0.17
	2.5%			1000.09	0.43
	0.05%	5000	20	1001.015	0.086
	2.5%			1000.54	0.14
Triangular $T_x=1000.8105\mu s \pm 0.0005\mu s$	0.05%	2500	40	1000.93	0.24
	2.5%			1000.063	0.24
	0.05%	5000	40	1001.81	0.37
	2.5%			1000.06	0.34
	0.05%	5000	20	1000.86	0.18
	2.5%			1000.45	0.11
Square $T_x=1000.8105\mu s \pm 0.0005\mu s$	0.05%	2500	40	1000.94	0.24
	2.5%			1000.87	0.33
	0.05%	5000	40	1000.44	0.49
	2.5%			1000.45	0.49
	0.05%	5000	20	1000.82	0.29
	2.5%			1000.84	0.23

TABLE III  
NUMBER OF MEASUREMENTS IN 5 min USING  $f_s = 50$  kS/s

N	Embedded function	Author function
500	16189	5083
1000	9664	2705
2500	5074	1055

does not influence the visualization quality because the resulting rate is, in any case, higher than the human-eye bandwidth.

## V. CONCLUSION

Most of the scope period measurement functions are based on the zero-crossing algorithm, which is robust and fast but completely wrong when signals have more than one zero crossing in the period. In this paper, a solution to enhance the period-measurement capability of scopes has been presented. A measurement procedure proposed by Schoukens *et al.* in [13] was analyzed and suitably modified to be adapted to real-time exigencies of oscilloscopes. Then, it has been implemented in MATLAB and included in the set of measurement functions of the LeCroy WaveMaster 8620 A. The procedure, based on the autocorrelation function, proved to be accurate for any signal

waveform. Even though the new measurement function requires a significant additional burden, the scope response time remains acceptable. Future developments will be devoted to further optimization of the software in order to reduce the execution time.

## ACKNOWLEDGMENT

The authors wish to thank Ing. A. Giunchino for his help in the procedure implementation of the oscilloscope software.

## REFERENCES

- [1] Tektronix, *Digital Storage Oscilloscopes TDS6000 & TDS7000 Series*. [Online]. Available: <http://www.tektronix.com>
- [2] LeCroy, *Scopes WaveMaster 8000A Series*. [Online]. Available: <http://www.lecroy.com>
- [3] Tektronix, *CSA7000B Series & TDS7000B Series Instruments User Manual*. [Online]. Available: <http://www.tektronix.com>
- [4] LeCroy, *WaveMaster Series DDA-5005A Series User Manual*. [Online]. Available: <http://www.lecroy.com>
- [5] O. Valiviita, S. Ovaska, and S. J. Vainio, "Polynomial predictive filtering in control instrumentation: A review," *IEEE Trans. Ind. Electron.*, vol. 46, no. 5, pp. 876–888, Oct. 1999.
- [6] J. G. Proakis and M. Salehi, *Communication Systems Engineering*. Englewood Cliffs, NJ: Prentice-Hall, 1994.
- [7] N. Geckinli and D. Yavuz, "Algorithm for pitch extraction using zero-crossing interval sequence," *IEEE Trans. Acoust., Speech, Signal Process.*, vol. ASSP-25, no. 6, pp. 559–564, Dec. 1977.
- [8] J. F. Chicaro, "A new algorithm for improving the accuracy of periodic signal analysis," *IEEE Trans. Instrum. Meas.*, vol. 45, no. 4, pp. 827–831, Aug. 1996.
- [9] R. Sudhakar, R. Agarwal, and S. D. Roy, "Frequency estimation based on iterated autocorrelation function," *IEEE Trans. Acoust., Speech, Signal Process.*, vol. ASSP-33, no. 1, pp. 70–76, Feb. 1985.
- [10] M. Lahat, R. Niederjohn, and D. Krubsack, "A spectral autocorrelation method for measurement of the fundamental frequency of noise-corrupted speech," *IEEE Trans. Acoust., Speech, Signal Process.*, vol. ASSP-35, no. 6, pp. 741–750, Jun. 1987.

- [11] H. Kobayashi and T. Shimamura, "A weighted autocorrelation method for pitch extraction of noisy speech," in *Proc. IEEE Int. Conf. Acoustics, Speech, and Signal Processing (ICASSP)*, Istanbul, Turkey, Jun. 5–9, 2000, vol. 3, pp. 1307–1310.
- [12] H. W. Wong-Lam and M. Naley, "A robust and accurate algorithm for time measurements of periodic signals based on correlation techniques," *IEEE Trans. Instrum. Meas.*, vol. 50, no. 5, pp. 1181–1189, Oct. 2001.
- [13] J. Schoukens, Y. Rolain, G. Simon, and R. Pintelon, "Fully automated spectral analysis of periodic signals," *IEEE Trans. Instrum. Meas.*, vol. 52, no. 4, pp. 1021–1024, Aug. 2003.
- [14] LeCroy, *WaveMaster 8000A Series, Operator's Manual*, Mar. 2003.

**Maria Grazia D'Elia** was born in Salerno, Italy, in 1975. She received the M.S. degree in electronic engineering from the University of Salerno, Fisciano, Italy, in 2002. She is currently working toward the Ph.D. degree in information engineering at the University of Salerno.

Her current research interests include digital signal processing and measurement characterization.



**Consolatina Liguori** (M'99) was born in Solofra (AV), Italy, in 1969. She received the M.S. degree in electronic engineering from the University of Salerno, Fisciano, Italy, in 1993 and the Ph.D. degree from the University of Cassino, Italy, in 1997.

In 1997, she joined the Department of Industrial Engineering, University of Cassino, as an Assistant Professor in electrical measurements. Since 2001, she has been an Associate Professor in electrical and electronic measurements. In 2004, she joined the Department of Information Engineering and Electric

Engineering, University of Salerno. Her main research interests are in the fields of digital signal processing and image-based measurement systems and measurement characterization.



**Vincenzo Paciello** was born in Salerno, Italy, in 1977. He received the M.S. degree in electronic engineering from the University of Salerno, Fisciano, Italy, in 2002. He is currently working toward the Ph.D. degree in information engineering at the University of Salerno.

His current research interests include wireless sensor networks, instrument interfaces, and digital signal processing for advanced instrumentation.



**Antonio Pietrosanto** (M'99) was born in Napoli, Italy, in 1961. He received the M.S. and Ph.D. degrees in electrical engineering from the University of Napoli in 1986 and 1990, respectively.

In 1991, he became an Assistant Professor and, in 1999, an Associate Professor of electrical and electronic measurements at the University of Salerno, Fisciano, Italy. Since November 2001, he has been a Full Professor in electrical and electronic measurements at the University of Salerno. His scientific research interests are instrument fault detection iso-

lation and accommodation, digital signal and image processing for real-time diagnostic and process control, and fiber optic sensors.